JOURNAL OF MATERIALS SCIENCE 16 (1981) 1643–1653

The application of a new solidification heat flow model to splat cooling

T. W. CLYNE
Department of Materials, Swiss Federal Institute of Technology (EPFL), CH 1007 Lausanne Switzerland

A. GARCIA
Department of Mechanical Engineering, State University of Campinas (UNICAMP), Campinas SP, Brazil

This paper outlines how the virtual adjunct method (VAM) of Garcia, Clyne and Prates, describing heat flow in unidirectional solidification, may be applied to splat cooling processes. The model allows finite thermal resistance across the mould–metal interface and leads to explicit solutions which are mathematically exact. Examples are presented showing how the equations may be used to investigate the relationships between melt–substrate properties, operating parameters and local cooling conditions, with particular reference to the treatment of vitrification. A brief outline is given of how closely real systems are likely to conform to the boundary conditions under which the model must be applied. It is concluded that, while numerical treatments may be required if a given system is to be accurately modelled, the VAM equations should prove useful for general examinations of splat cooling characteristics and in assessing the expected effects of changes in design and operational features.

1. Introduction

There has in recent years been considerable interest in promoting very rapid cooling of (metallic) liquids. Following the original outline of the splat cooling principle [1], a number of experimental set-ups have been described [2–6], all of which depend on bringing a body of liquid metal rapidly into intimate surface contact with a massive substrate. Following the original discovery [7] that amorphous (glassy) structures could be produced at high cooling rates, extensive work has been carried out on the formation of glassy metals and a start has been made on their commercial exploitation [8, 9].

Treatments of the kinetics of atomic redistribution during nucleation of crystalline regions [10, 11] have revealed the importance of the local cooling rate $\dot{T}$ in controlling formation of glassy solid. Estimates of the form of the *TTT* curve corresponding to the start of crystallization [12, 13] may be used to deduce the critical cooling rate $\dot{T}_c$ necessary to avoid the "nose" of this curve and thus give rise to a glassy structure. A wide range of alloys have now been produced in glassy form (e.g. see Davies [14]) with estimated $\dot{T}_c$ values in the range of 10^2 to 10^8 K sec^{-1}. However, as Davies [14] has pointed out, the form of the thermal history over an appreciable temperature range may be important in deciding whether crystallization will be avoided, and this may be correlated with the time characteristics of different types of splat cooling process.

It is thus clearly important to be able to characterize the thermal behaviour of a splat cooling system from a knowledge of the operating conditions. However, while a number of heat-flow models [15–21] have been applied to contact conduction cooling with high heat-extraction rates, none can be said to combine acceptable generality with relative simplicity. Ruhl [17] has estimated via finite difference computations that, with a substrate of high thermal diffusivity, cooling

0022–2461/81/061643–11$03.10/0

is controlled by the thermal resistance of the interface for Biot numbers (Bi) below 0.015 and by that of the solidified layer for values above 30. In practice, the conditions during splat cooling are normally such that Bi falls between these two figures over much of the range (of melt thickness) which is of interest.

It follows that application to splat cooling should be limited to models capable of describing heat flow under mixed thermal control. This has until recently only been possible via techniques employing arbitrary functions to describe the heat flux or thermal profile [20, 21] (which involve lengthy integration procedures and which have been shown [22] to be inaccurate in certain regimes) or by numerical methods. However, a recent exact analytical model [23, 24] now allows explicit solution of the generalized case in which the interfacial heat transfer coefficient has a finite constant value. In this paper, the equations describing the freezing behaviour and thermal characteristics are presented and their application to splat cooling is demonstrated, using typical experimental conditions and materials of current interest in the examples. The nomenclature for the symbols employed is detailed in Appendix A.

2. Analytical solution

The new model is based on the mathematical expedient of representing the thermal resistance of the metal–mould interface by imaginary extra thicknesses of metal and mould material, and has been termed the virtual adjunct method (VAM). The mathematics of the basic model have been detailed [23, 24] for the zero super-heat case and only the principal equations are presented here, although they incorporate a minor development allowing finite pouring super-heat ($T_p - T_f$). Interface movement is described by the equation

$$t = \alpha S^2 + \beta S, \tag{1}$$

where

$$\alpha = \frac{1}{4a_s\phi^2} \tag{2}$$

and

$$\beta = \frac{c_s d_s}{\pi^{1/2}\phi \exp(\phi^2)\{M + \operatorname{erf}(\phi)\}h_i} \tag{3}$$

and the solidification constant ϕ is obtained by iteration from the following condition

$$\frac{\exp(-\phi^2)}{M + \operatorname{erf}(\phi)} = \frac{m(T_p - T_f)\exp(-n^2\phi^2)}{(T_f - T_0)\{1 - \operatorname{erf}(n\phi)\}} + \frac{\pi^{1/2} H \phi}{c_s(T_f - T_0)}. \tag{4}$$

The thermal characteristics of the process are represented by the following equations

$$T_m = T_0 + \frac{(T_f - T_0)M}{M + \operatorname{erf}(\phi)}\left[1 + \operatorname{erf}\left(\phi\frac{2\alpha NX - \beta}{2\alpha S + \beta}\right)\right]; \tag{5}$$

$$T_s = T_0 + \frac{(T_f - T_0)}{M + \operatorname{erf}(\phi)}\left[M + \operatorname{erf}\left(\phi\frac{2\alpha X + \beta}{2\alpha S + \beta}\right)\right]; \tag{6}$$

$$T_L = T_p - \frac{(T_p - T_f)}{l - \operatorname{erf}(n\phi)}\left[1 - \operatorname{erf}\left(n\phi\frac{2\alpha X + \beta}{2\alpha S + \beta}\right)\right]. \tag{7}$$

The thickness of the metal and mould side adjuncts are given respectively by the two equations below

$$S_0 = \frac{2\phi k_s}{\pi^{1/2}\exp(\phi^2)h_i\,[\operatorname{erf}(\phi) + M]} \tag{8}$$

and

$$E_0 = \frac{S_0}{N\phi}\left[\ln\frac{2N\phi k_m M}{\pi^{1/2}h_i\{\operatorname{erf}(\phi) + M\}S_0}\right]^{\frac{1}{2}}. \tag{9}$$

The case of $M \to 0$ corresponds to a mould acting as a perfect heat sink at T_0, and the form of the model in this limit has been outlined [25]. Thermophysical data employed in the calculations (which are in certain cases of necessity rather approximate) are given in Table AI in Appendix B.

3. Conventional solidification

A problem is encountered in applying heat-flow models to rapid solidification of thin foils in that the experimental data required for ratification are difficult to obtain by direct measurement (although attempts have been made, e.g. see Jones [19]) and may also be imprecise when inferred from solidification structure. However, the validity of the VAM model has been checked over a range of conditions (involving less efficient interfacial heat transfer than is met in splat cooling), including solidification through regimes of mixed thermal control. During conventional casting, h_i would normally fall in the range 10^2 to 10^4 $W m^{-2} K^{-1}$, depending primarily on mould surface and configurational factors [26, 27]. (This compares with typical estimates of 10^4 to $10^5 W m^{-2} K^{-1}$ for pressure die casting [28] and 10^4 to 5×10^6 $W m^{-2} K^{-1}$ for a range of splat cooling processes [14, 19, 29].)

Values of h_i during conventional casting are often such that estimates of the location of the regime of mixed thermal control indicate this to

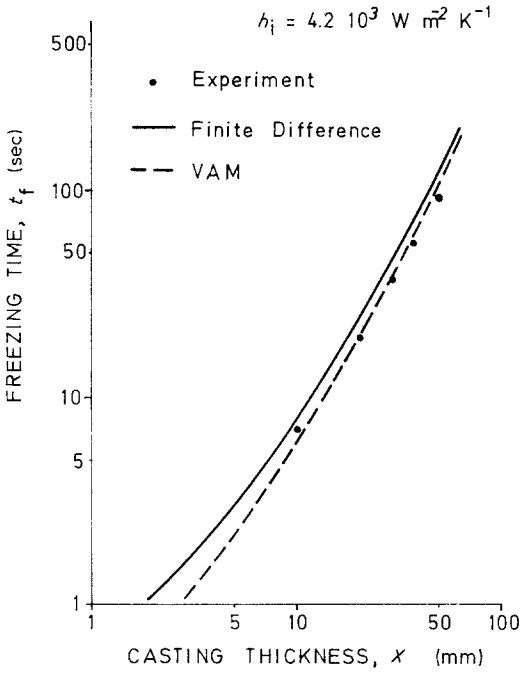

Figure 1 Comparison between experimental dipstick measurements [23], and theoretical curves from the VAM model and from finite difference computations.

lie within a range of thickness solidified which is conveniently monitored with laboratory apparatus. For example, Fig. 1 shows experimental growth data for lead freezing against a massive steel mould with a polished surface, and the value of Bi varied in this case from about 1 to 10 over the thickness range monitored. Also shown are the predictions of the VAM model and of a finite difference programme, both of these having been applied using the value of h_i obtained by a previously described technique [24, 30].

4. Splat cooling of thin foils

A number of splat cooling processes have been developed and their characteristics differ slightly in some cases. Application of the VAM model as described in the following examples is quite general, subject to the constraints of unidimensional heat flow and invariant interfacial conductance for the duration of the quench (see Section 4.3). These boundary conditions would be expected to hold quite accurately for many splat cooling processes. An example of the type of configuration that can be modelled is given in Fig. 2, which shows a schematic illustration of the thermal profile during quenching between a pair of contrarotating drums; such as those used in the

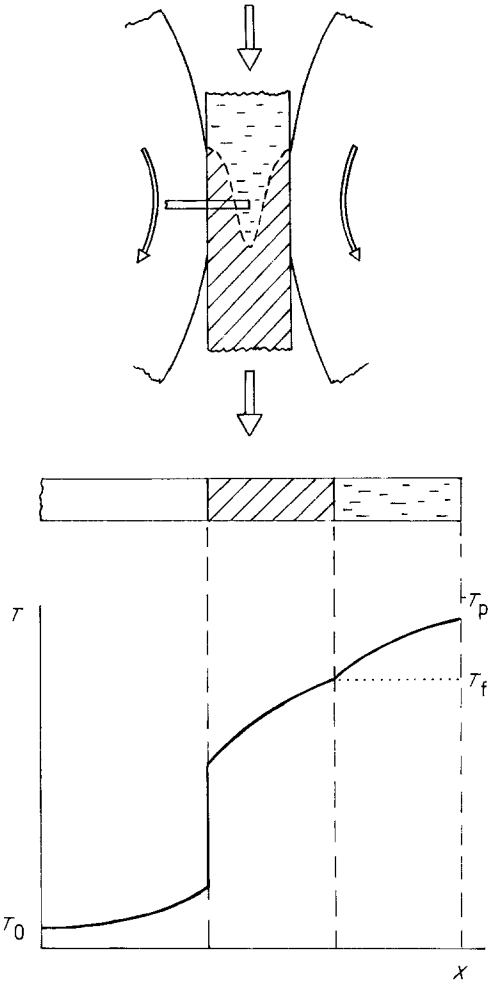

Figure 2 Schematic illustration of the thermal profile through the thickness of a ribbon foil during twin-drum quenching.

commercial production of ribbon foils of glassy metal [9] (and similar in principle to the Hunter process for strip casting of aluminium [31]). Data are first presented from calculations involving rapid crystallization of pure nickel. The complications that arise on introducing the possibility of avoiding crystallization are then illustrated with reference to two nickel-based alloys that can be vitrified with different degrees of difficulty.

4.1. Interfacial contact

An indication of how freezing might be expected to progress during splat cooling of a foil of Ni is given by Fig. 3, which shows growth curves for h_i values covering much of the range expected in practice. The relatively large separation between these curves implies that the exact value of h_i is important in this range for foil thicknesses of

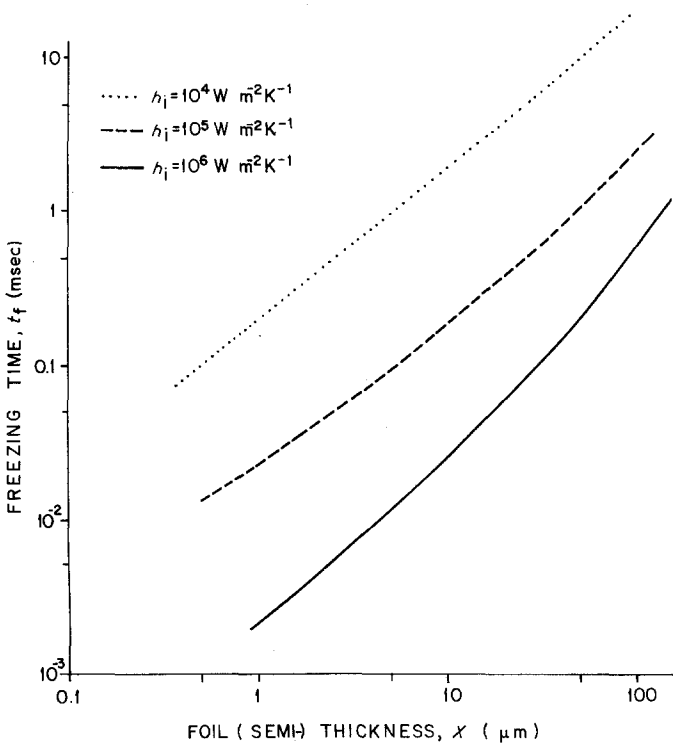

Figure 3 Predicted curves for the dependence of freezing time on distance from the foil–substrate interface for three interfacial heat transfer conditions. Data for Ni with zero melt superheat in contact with a copper substrate initially at 290 K.

interest ($\lesssim 100\,\mu$m). It emerges as a general conclusion from modelling a range of situations that efforts to make (even small) increases in h_i (towards a figure around $10^7\,W\,m^{-2}\,K^{-1}$) should be worthwhile in terms of increasing the cooling efficiency, particularly for thin foils.

4.2. Substrate

Taking freezing of Ni with $h_i = 10^5$ as a reference case, the effect of changing the nature of the substrate is shown in Fig. 4. Copper has the highest heat diffusivity (a measure of the heat extracting efficiency) of all metals and it can be seen that, in terms of freezing a thin Ni foil, it has an effect almost equivalent to that of a perfect heat sink (maintained at room temperature). The figure also shows that allowing the substrate to become hot, or substituting it with a steel one, have only small effects on the freezing behaviour. This would seem to imply that, with a rotating drum system for example, cooling of the drums, and the material of which they are constructed, are not of critical importance. However, two points should be noted in this context. Firstly, the freezing behaviour is in this case insensitive to the nature of the substrate primarily because of the high melting temperature of Ni (1725 K), which is considerably higher than, for example, those of the Ni alloys used in glassy foils. Secondly, the curves give no indication of the rates of cooling of different points after the fusion temperature has been passed, which is essentially what controls glass formation. In practice, this is much more sensitive to substrate characteristics and this point is brought out later (see Fig. 9, Section 4.3).

The model can also be used to investigate temperature changes occurring within the substrate. (This might have practical applications, such as in estimating the minimum thickness of a copper layer on a stainless steel drum required to give the same heat extraction efficiency as a copper drum.) The end point thermal profiles for freezing of a Ni foil of (semi-) thickness 20 μm on a Cu substrate are shown in Fig. 5 for 3 values of h_i. It is clear that the depth to which the substrate becomes heated up during freezing of a foil of given thickness will depend quite strongly on the heat transfer coefficient.

4.3. Glass formation

In treating vitrification rather than crystallization, it is necessary to change the boundary conditions of the problem, although the same basic heat-flow equations remain valid. While vitrification does not take place at a well-defined temperature, it is convenient to treat the transformation as if it

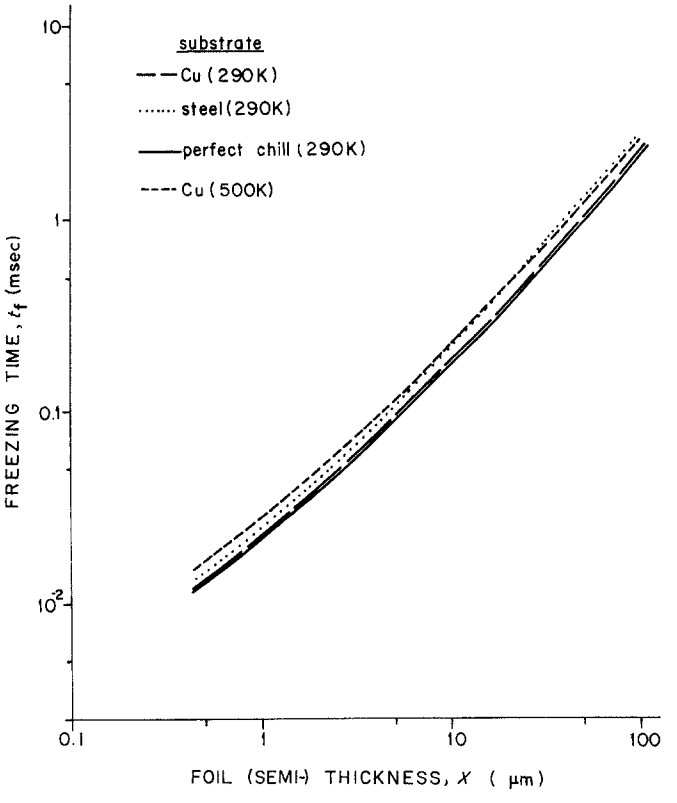

Figure 4 Growth curves for Ni freezing against different types of substrate with $h_i = 10^5$ W m^{-2} K^{-1}.

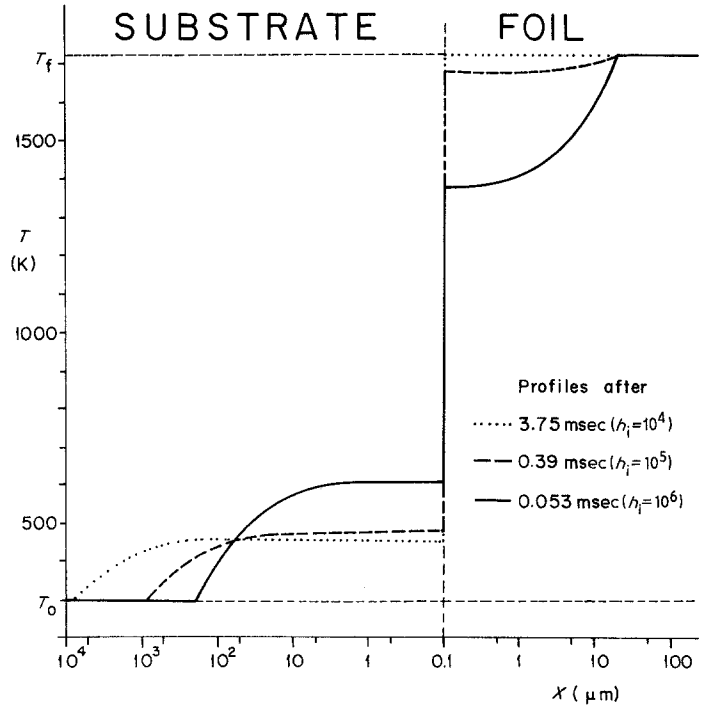

Figure 5 Thermal profiles across the region near the substrate–foil interface, after the different periods necessary for the crystallization front in a Ni foil to advance 20 μm, when in contact with a Cu substrate under different thermal contact conditions.

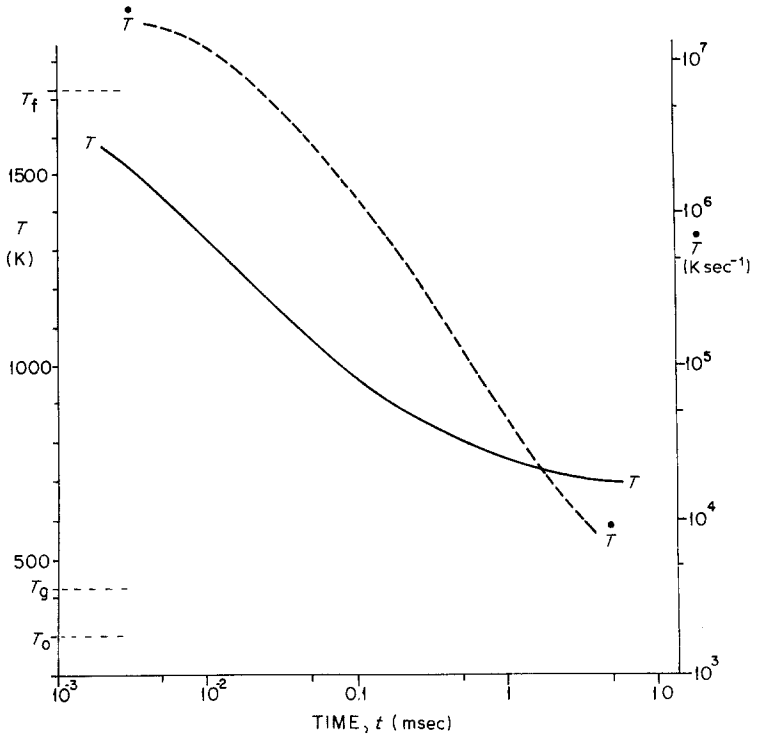

Figure 6 Thermal history and local cooling rate curves referring to a point 1 μm below the surface of a Ni foil being cooled (without crystallization) against a Cu substrate with $h_i = 10^6$ W m^{-2}K^{-1}.

occurred at the glass transition temperature T_g [which can be measured experimentally by differential scanning calorimetry (DSC)]. This is not an intrinsically important point in terms of the analysis, in that there is now neither evolution of latent heat nor significant changes in thermophysical properties on passing the transformation temperature. It may also be noted that the temperature corresponding to the nose of the *TTT* curve could be of more significance in terms of the thermal behaviour: this will in general be appreciably above T_g, although exact values are difficult to obtain.

The simplest way to apply the model to vitrification is to set T_f as T_g and use the melting point as T_p (pouring temperature). The predicted growth behaviour then describes the progress of an isotherm corresponding to the region where vitrification is assumed to be occurring. However, this will in many cases involve incorporating a large super-heat, and two points should be noted about use of the model in this case. Firstly, because the melt is assumed to be semi-infinite in extent, errors may arise due to the heat flux arriving from material which does not exist in the actual experimental set-up. (This effect could also introduce errors into predicted thermal histories with low super-heat, although the growth equations remain accurate.) Secondly, the model incorporates a boundary condition that the metal surface is instantaneously brought to its transformation temperature T_f on contact with the mould, which could be unrealistic with a large pouring superheat. (This potential source of error can be eliminated by setting $T_p = T_f$ = melting point, and using only the thermal history, Equations 6 and 7, to examine movement of the vitrification isotherm; although this approach involves extended calculation.) The errors introduced via these two effects should not, in general, be very pronounced, however, (and would tend to be in opposite directions) so that the thermal characteristics illustrated in the following figures should be at least qualitatively correct.

Fig. 6 shows the thermal history for a point 1 μm from the surface of a Ni melt brought into good thermal contact ($h_i = 10^6$) with a copper substrate (and assuming no latent heat evolution or change in thermophysical properties). Although the predicted cooling rates are initially quite high, it is clear that it would be very difficult to approach the estimated [12, 14] value of $\dot{T}_c$, which $\sim 3 \times 10^{10}$ K sec^{-1}. It may in any event be noted that the system will tend to a temperature T_i which is above T_g (although it might be lower with a melt of finite thickness). The graph suggests

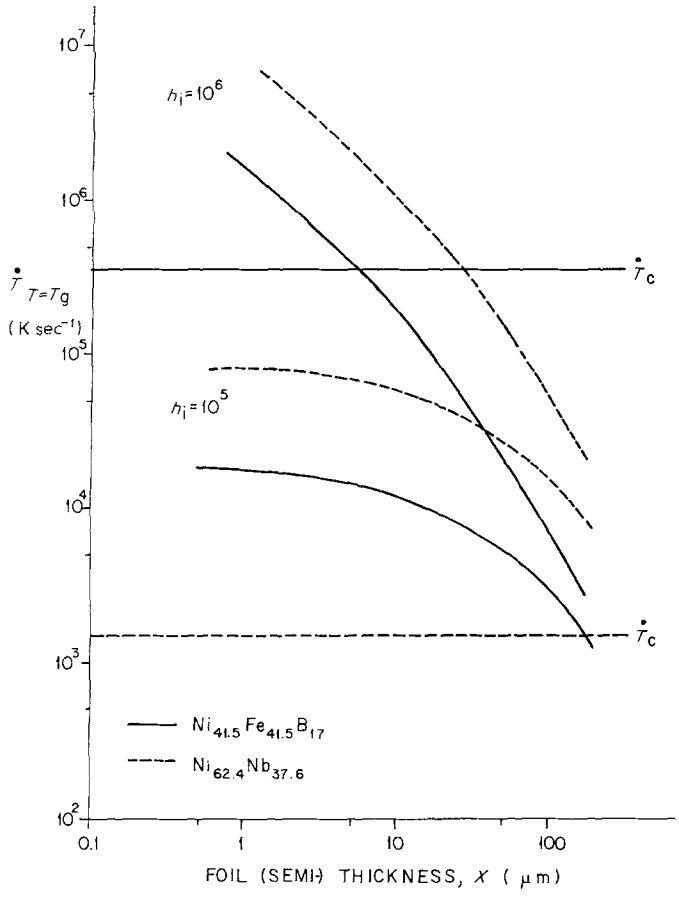

Figure 7 Through-thickness variations in local cooling rate on passing T_g (see Appendix B for thermophysical data) for two glass-forming alloys cooling against a copper substrate with two h_i values. Also shown are estimated $\dot{T}_c$ values for the alloys concerned.

that it would be extremely difficult to vitrify even a very thin foil of pure Ni, and this is borne out by practical experience (e.g. see Davies [12]).

Glass-forming alloys generally have compositions corresponding to deep (eutectic) troughs in the phase diagram and viscosities that increase rapidly with falling temperature (to give relatively high T_g values). Fig. 7 shows how the cooling rate on passing the T_g concerned depends on distance from the surface and the value of h_i. Curves are shown for two glass-forming alloys and may be compared with the respective estimated $\dot{T}_c$ values [14]. In practice the NiNb alloy is an easy glass-former and this is clearly consistent with the data shown: the NiFeB alloy is more difficult to vitrify, and this is compatible with the predicted importance of the exact value of h_i, apparent from the figure. It should be noted, however, that it would not be necessary for $\dot{T}_c$ to be exceeded all the way down to T_g in order to avoid the start of crystallization curve, so that the difficulty of vitrification is probably somewhat exaggerated in this figure.

It is important to note that a simple examination of cooling rates, such as that of Fig. 7, takes no account of whether thermal contact with the mould remains efficient long enough for the vitrification temperature to be passed at any given point in the foil. This depends in practice on the details of the process: for example, it has been estimated [14] that good thermal contact is maintained for a shorter period with twin-roll quenching than with melt spinning (before the foil starts to leave the substrate, causing a sharp fall in h_i). The dwell period, t_d, before this drop in interfacial conductance, has been estimated [14] to be in the broad neighbourhood of 1 msec for a typical continuous process and Fig. 8 demonstrates that this factor could be significant in determining the thickness of a NiFeB foil that could be vitrified (and again illustrates the importance of the exact value of h_i). Points further from the surface than that vitrified within the period t_d might still freeze with a glassy structure, of course, but this will depend on the details of the subsequent cooling conditions.

Finally, Fig. 9 demonstrates that the nature of

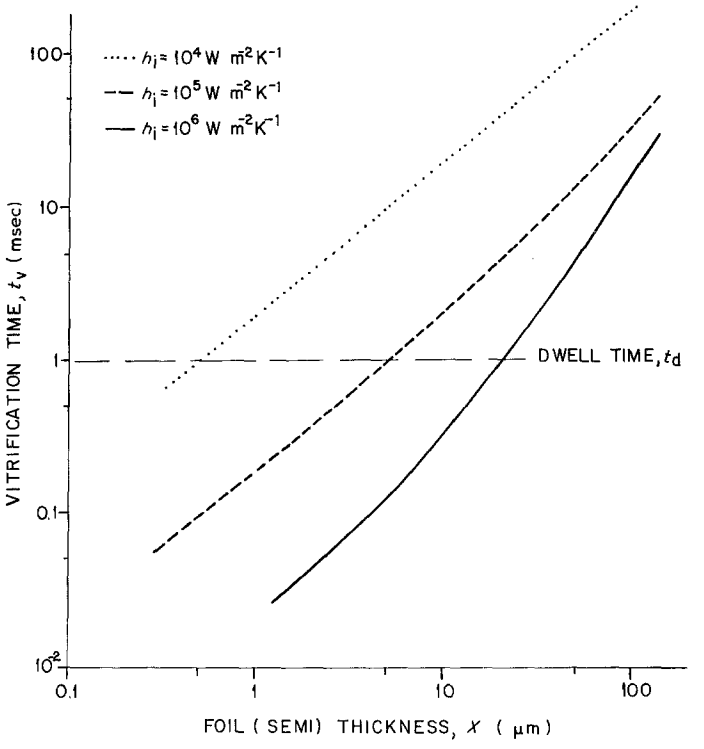

Figure 8 Growth curves showing the advance of the "vitrification isotherm" ($T_g = 720$ K) for the $Ni_{41.5}Fe_{41.5}B_{17}$ alloy cooling against a Cu substrate (initially at 290 K) with $3h_i$ values. Also shown is an indication of what the dwell time (for which h_i is maintained at the value concerned) might be depending on the details of the experimental set-up.

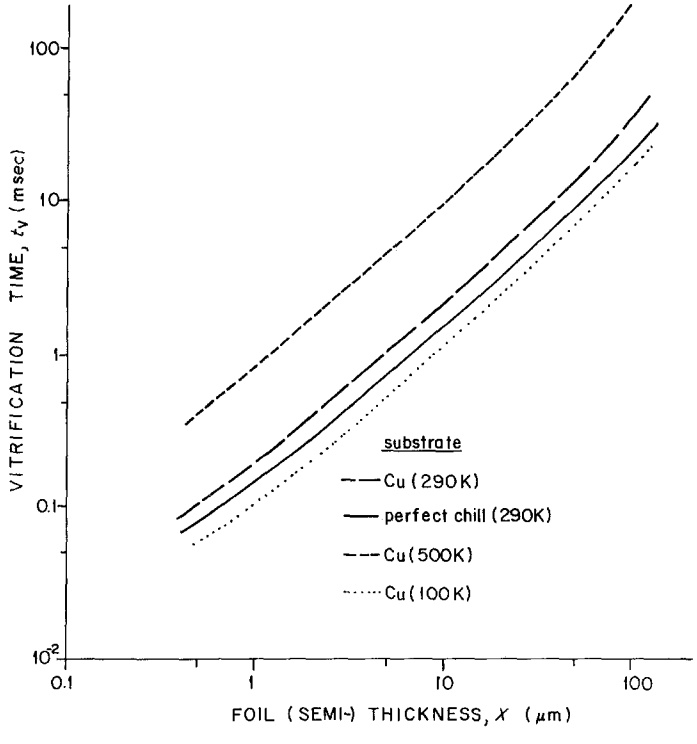

Figure 9 Vitrification isotherm advance curves for the $Ni_{41.5}Fe_{41.5}B_{17}$ alloy cooling against different substrates with $h_i = 10^5$ W m^{-2} K^{-1}.

the substrate is very important in quenching aimed at vitrification. This figure shows the progression of the T_g isotherm for the NiFeB glass with an h_i of $10^5\ W m^{-2} K^{-1}$. It is clear that a copper substrate initially at ambient temperature acts almost like a perfect heat sink. However, the quenching efficiency falls quite sharply if the copper is allowed to heat up beforehand: so that effective (water) cooling of a rotating drum might be very important (depending on the thermal masses involved). It could be inferred, however, that the further improvement in quenching efficiency that results from cooling below ambient temperature (e.g. with liquid nitrogen) might not be sufficient to warrent the increased complexity of the experimental set-up. It is also essential that the drum is of a material with high heat diffusivity. Vitrification would be impossible for the case shown if a steel substrate at ambient temperature were used, as the system would tend to a temperature above T_g. These results may be contrasted with the case of crystallization of a Ni foil (Fig. 4), for which the nature of the substrate has little effect on the freezing behaviour.

5. Summary and conclusions

It is clear that the VAM model can given a comprehensive description of freezing processes such as those involved in certain types of splat quenching. Some examples have been given which have demonstrated how the analytical solutions may be applied to investigate different aspects of rapid cooling against a massive substrate by unidimensional heat transfer.

Application of the model to normal solidification has been demonstrated both for conventional casting (for which good agreement is observed with experimental data) and for rapid quenching. The way in which the boundary conditions should be modified to deal with vitrification was illustrated with reference to two glass-forming alloys. In all cases, the model predictions satisfactorily covered the transition from interface-dominated to conduction-controlled heat-flow.

It has been clearly revealed that, for the expected ranges of splat thickness and thermophysical conditions, the exact value of the interfacial heat transfer coefficient is of considerable importance. Examples have also been given illustrating ways in which the effect of the nature of the substrate can be investigated. Substrate characteristics have been shown to be important in the formation of glassy foils: material with high heat diffusivity should be used and substrate cooling may contribute significantly to the ease of vitrification for continuous production processes.

Finally, the flexibility of the model has been demonstrated by presenting various types of thermal history predictions. These are expected to be useful in determining vitrification conditions. Comparisons have been presented demonstrating the importance of both material properties (such as critical cooling rate $\dot{T}_c$) and operational parameters (such as foil–substrate dwell time t_d) in relation to the thermal characteristics of the system.

While the model is exact mathematically, the boundary conditions imposed may in some cases not correspond well to the actual physical constraints and this could give rise to significant errors. While the model is superior in this respect to other analytical solutions, numerical treatments can often be made to conform more accurately to the physical conditions in a given, well characterized set-up. However, the model should be useful for more general calculations (and is particularly suited to those involving continuous foil production). It may be manipulated to provide insights into the relationships between material properties, interfacial heat transfer and local cooling conditions and may thus come to constitute a useful tool for workers studying rapid freezing of metallic melts.

Acknowledgements

This study was undertaken over a period during which financial support was provided by the Aluminium Fonds Research Fund and by FAPESP (the Scientific Research Foundation of the State of Sao Paulo, Brazil).

Appendix A

Nomenclature

(a) Parameters

- a thermal diffusivity $= k/c\,d$ ($m^2\ sec^{-1}$).
- Bi Biot number $= h\,S/k$ (dimensionless).
- c specific heat ($J\,kg^{-1}\,K^{-1}$).
- d density ($kg\,m^{-3}$).
- E_0 thickness of mould side adjunct (m).
- h Newtonian heat transfer coefficient ($W\,m^{-2}\,K^{-1}$).
- H latent heat of fusion/transformation ($J\,kg^{-1}$).
- k thermal conductivity ($W\,m^{-1}\,K^{-1}$).
- m constant of metal $= (k_L c_L d_L / k_s c_s d_s)^{1/2}$ (dimensionless).

M constant of metal–mould system $= (k_s c_s d_s / k_m c_m d_m)^{1/2}$ (dimensionless).
n constant of metal $= (a_s/a_L)^{1/2}$ (dimensionless).
N constant of metal–mould system $= (a_s/a_m)^{1/2}$ (dimensionless).
S thickness of solidified metal (m).
S_0 thickness of metal side adjunct (m).
t time (sec).
T Temperature (K).
$\dot{T}$ cooling rate (K sec^{-1}).
X distance from metal–mould interface (m).
ϕ solidification constant (dimensionless).

(b) Subscripts

c critical.
d dwell.
g glass transition.
f fusion–freezing.
i metal–mould interface.
L liquid.
m mould.
p pouring.
s solid.
V vitrification.
O mould (original).

Appendix B Thermophysical properties

TABLE AI Thermophysical properties

Property	Material					
	Splat				Substrate	
	Ni		$Ni_{41.5}Fe_{41.5}B_{17}$ Liquid (glass)	$Ni_{62.4}Nb_{37.6}$ Liquid (glass)	Copper	Steel
	Liquid (glass)	Solid				
k (W m^{-1} K^{-1})	30	60	12	12	400	16
c (J kg^{-1} K^{-1})	620	600	620	550	390	500
d (kg m^{-3})	8.5×10^3	8.9×10^3	7.5×10^3	8.4×10^3	9×10^3	7.9×10^3
H (J kg^{-1})	–	3×10^5	–	–	–	–
T_f (K)	1725	1725	1352	1442	–	–
T_g (K)	425	–	720	945	–	–
$\dot{T}_c$ (K sec^{-1})	3×10^{10}	–	3.5×10^5	1.4×10^3	–	–

References

1. P. DUWEZ, R. H. WILLENS and W. KLEMENT, *J. Appl. Phys.* **31** (1960) 1136.
2. P. DUWEZ and R. H. WILLENS, *Trans. Met. Soc. AIME* **227** (1963) 362.
3. P. PIETEROKOWSKI, *Rev. Sci. Instr.* **34** (1963) 445.
4. R. ROBERGE and H. HERMAN, *Mater. Sci. Eng.* **3** (1968) 62.
5. R. POND and R. MADDIN, *Trans. Met. Soc. AIME* **245** (1969) 2475.
6. H. S. CHEN and C. E. MILLER, *Rev. Sci. Instr.* **41** (1970) 1237.
7. W. KLEMENT, R. H. WILLENS and P. DUWEZ, *Nature* **187** (1960) 869.
8. N. DECRISTOFARO and C. HENSHEL, "Metglas Brazing Foil", paper presented at the 9th International AWS-WRC Brazing Conference, New Orleans, April, 1978 (see also *Welding J.* July, 1978).
9. Allied Chemicals, "Metglas" information publications (available from: Metglas Products, 7 Vreeland Rd, Florham Pk, NJ 07932) (1980).
10. D. R. UHLMANN, *J. Non-Cryst. Sol.* 7 (1972) 337.
11. H. A. DAVIES and B. G. LEWIS, *Scripta Met.* 9 (1975) 1107.
12. H. A. DAVIES, *Phys. Chem. Glasses* **17** (1976) 159.
13. H. A. DAVIES, J. AUCOTE and J. B. HULL, *Scripta Met.* 8 (1974) 1179.
14. H. A. DAVIES, Proceedings of the 3rd International Conference on Rapidly Quenched Metals, Vol. I, paper A1, (The Metals Society, London, 1978).
15. H. JONES, *Mater. Sci. Eng.* 5 (1969/70) 1.
16. P. H. SHINGU and R. OZAKI, *Metall. Trans.* **6A** (1975) 33.
17. R. C. RUHL, *Mater. Sci. Eng.* 1 (1967) 313.
18. K. MIYAZAWA and J. SZEKELY, *Metall. Trans.* **10B** (1979) 349.
19. H. JONES, *Rep. Prog. Phys.* **36** (1973) 1425.
20. A. W. D. HILLS, *J. Iron Steel Inst.* **203** (1965) 18.
21. R. M. TIEN, *Trans. TMS-AIME* **233** (1965) 1887.
22. A. S. PEDRAZA, S. HARRIAGUE and D. FAINSTEIN-PEDRAZA, *Metall. Trans.* **11B** (1980) 321.
23. A. GARCIA, T. W. CLYNE and M. PRATES, *ibid.* **10B** (1979) 85.
24. T. W. CLYNE and A. GARCIA, *Int. J. Heat Mass Transfer* **23** (1980) 773.
25. A. GARCIA and M. PRATES, *Metall. Trans.* **9B** (1978) 449.
26. L. J. D. SULLY, *Trans. AFS* **84** (1976) 735.
27. A. MORALES, M. E. GLICKSMAN and H. BILONI "Solidification and Casting of Metals" (The Metals

Society, London, 1979) p. 184.
28. S. HONG, D. G. BACKMAN and R. MEHRABIAN, *Metall. Trans.* **10B** (1979) 299.
29. H. A. DAVIES, private communication (1980).
30. A. GARCIA and T. W. CLYNE, Proceedings of the Conference on Solidification Technology in the Foundary and Casthouse, University of Warwich, September, 1980.
31. E. F. EMLEY, *Int. Met. Rev.* **21** (1976) 75.

Received 19 June and accepted 24 November 1980.